Ilkogretim Online - Elementary Education Online, 2021; Vol 20 (Issue 3): pp. 3189-3197
http://ilkogretim-online.org
doi: 10.17051/ilkonline.2021.03.330

Analysis Of Soft Pneumatic Actuators With Different Cross-Section Of Air Chambers

Narendra Gariya*[1], Mohd Faisal[2], Ronit Singh Raghuvanshi[3], Rohit Raizada[4], Dr. Taranath[5]

[1,2,3,4] Department of Mechanical Engineering, Graphic Era Deemed To Be University, Dehradun
[5] Assistant Professor, Department of Computer Science and Engineering, Graphic Era Hill University, Dehradun
Corresponding Author Email Id: navigk05@gmail.com

Abstract. Soft robots are far more adaptable than conventional rigid robots. They have high flexibility, infinite degree of freedom, and their compliant nature makes them the best option for different industrial, surgical, and healthcare applications. The efficiency of a soft can be estimated by the performance of the soft actuators. Soft pneumatic actuators (SPAs) are the most common and highly utilized soft actuators because of their high low weight and high output force. In this study, three different SPAs, single chamber SPA with rectangular cross-section, multi-chamber SPA with square air chambers, and multi-chamber SPA with circular air chambers, have been modeled and analyzed using the finite element analysis (FEA) theory. The results concluded that the multi-chamber SPA creates large bending as compared to the single chamber SPA under similar loading and boundary conditions. However, the SPA with circular air chambers creates large bending as compared to the SPA with square air chambers.

Keywords: SPA; FEA; Air chamber; Bending; Silicone rubber.

1. Introduction

Recently, the demand for soft materials in the fabrication of soft robots has increased because of which the soft robotic community has seen many advancements. The main reason behind this is the advantages of soft robots over conventional rigid robots. The main advantage of soft robots is their high flexibility and compliant behavior. Soft robots allow us to mimic the functioning of various living organisms and their muscles [1]. Moreover, they provide safer interaction as compared to rigid robots while working with humans. The effectiveness of the soft robot can be estimated by the performance of the soft actuators. There are various types of soft actuators such as electroactive polymer actuators, fluidic (pneumatic and hydraulic) actuators, material jamming actuators, and

many more. Soft pneumatic actuators (SPAs) are the most frequently utilized soft actuators and are simple in design [2].

However, SPAs developed with elastomeric or hyperelastic materials such as the ecoflex [3], dragon skin [4]. Elastosil [5], and smoothsil [6] are subjected to large deformation. Hence, it is very difficult to model these materials using the stress-strain curve. Various techniques or theories have been applied to design and control the SPAs such as the Cosserat rod theory [7], piecewise constant curvature theory [83], variable-strain theory [59], and Euler Bernoulli beam theory [10]. Other theories such as reinforcement learning and neural network are based on data-driven techniques. Many researchers use the finite element analysis (FEA) technique to model hyperelastic material. [11] uses the FEA technique to identify the displacement and force generated by the SPAs. Some researchers carried out the modeling of the fiber-reinforced SPAs using the theory of continuum mechanics [12, 13]. Another theory splits the actuators into small segments and then studies the bending of segments individually and adds them to evaluate the bending of the whole actuator [14].

In this study, three different SPAs are modeled and are considered to have properties of natural rubber. All three SPAs are analyzed using the FEA theory in Abaqus. Two different hyperelastic material models the Neo-Hookean and the Ogden have been considered and the material constants are taken from the literature. All three SPAs are analyzed for similar boundary and loading conditions.

2. Modeling of the SPAs

The SPA has been modeled using the computer-aided design (CAD) software – CATIA V5. The three different SPA has been modeled based on the dimension obtained from the literature [15]. All three SPA models have equal length (120 mm), width (20 mm), and height (20 mm). The three different SPA models are –

- **Single chamber SPA with rectangular cross-section**

This type of SPA also known as plane SPA has a single air chamber for the pneumatic actuation. The model of the single chamber SPA is shown in the figure 1.

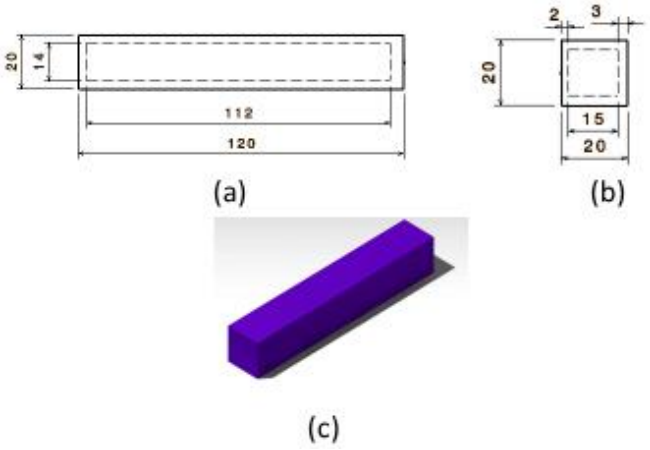

Figure 1. (a) Front view, (b) Side view, and (c) Isometric view of the single chamber SPA

Figure 1 depicts that the length and the width of the single chamber are 112 mm and 14 mm, respectively. The top wall is 2 mm thick while the side walls are 3 mm thick. The bottom layer also known as the strain limiting layer is 3 mm thick. The stiffness of the top wall is lower than the side and the bottom wall due to which the SPA bents during the pneumatic actuation.

- **Multi-chamber SPA with square air chambers**

The multi-chamber SPA has multiple air chambers for the pneumatic actuation. The air chambers are of square cross-section as shown in the figure 2.

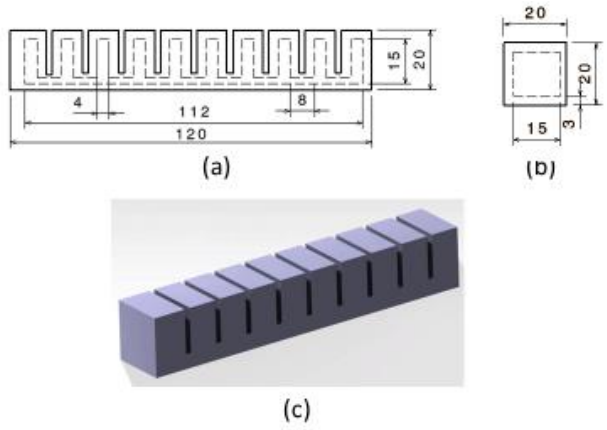

Figure 2. (a) Front view, (b) Side view, and (c) Isometric view of the multi-chamber SPA with square air chambers

Figure 2 depicts that the SPA has a total of ten air chambers for the pneumatic actuation. The stiffness of the top wall (2 mm thick) is lower than the bottom wall (3 mm thick). The gap between the two adjacent air chamber is 2 mm while the side walls are of 3 mm thickness.

- **Multi-chamber SPA with circular air chambers**

The modeled SPA have ten air chambers for actuation with a circular cross-section. The circular cross-section of the air chamber is of 5 mm radius as shown in the figure 3.

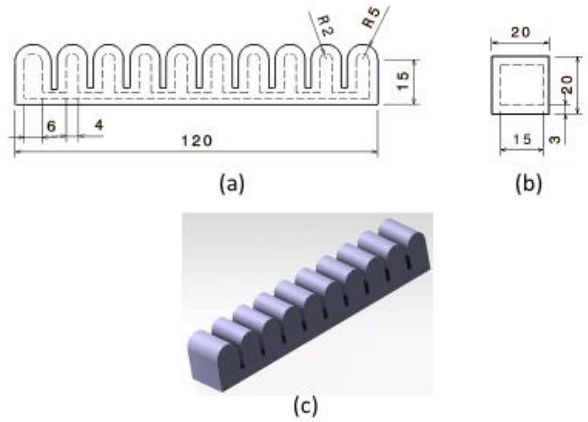

Figure 3. (a) Front view, (b) Side view, and (c) Isometric view of the multi-chamber SPA with circular air chambers

Figure 3. depicts that the modeled SPA has ten air chambers of circular cross-section. The 2 mm gap between the two adjacent air chamber allowed the higher bending of the SPA. In this model, the top, side, and bottom walls are of 3 mm thickness.

3. Finite Element Analysis (FEA)

Various types of materials are there in nature such as steel, copper, and aluminum which come under the elastic category. Under loading, these materials are subjected to yielding before the plastic deformation and then fracture. Ceramic materials go under linear elastic deformation without plastic deformation before fracture. All materials are not elastically linear, some are subjected to elastic strains more than 100% during loading and fail without plastic deformation. The materials are known as hyperelastic materials. Natural rubber or silicone rubber comes under the category of hyperelastic material. The stress-strain relationship for these types of material is highly non-linear and requires strain energy density potential or function. For evaluating the large strain behavior of these material, different hyperelastic material models are available such as Neo-Hookean, Yeoh, Mooney-Rivlin, Polynomial, and the Ogden model.

For the analysis of modeled SPA, the Neo-Hookean, and the Ogden hyperelastic model has been considered. The Neo-Hookean model is the simplest model that requires only two parameters, that is shear behavior term, and compressibility term. If the term is non-compressible then there is only one term (shear behavior) required for the strain energy density function. The Ogden model is best for the soft materials subjected to the higher volumetric strains.

For the study, the natural rubber has been considered from the literature [15] and the strain energy density function for the Neo-Hookean and the Ogden model is given by [16],

Neo-Hookean Model: The strain energy density function (W) is defined by,

$$W = C_{10}(I_1^- - 3) + \frac{1}{D_1}(J_{el} - 1)^2 \qquad (1)$$

Where I_1^- is the first deviatoric strain invariant, D_1, and C_{10} are the material constants, and J_{el} is the elastic volume ratio.

Ogden Model: The strain energy density function (W) is provided as,

$$W = \sum_{i=1}^{N} \frac{2\mu_i}{\alpha_i^2}\left(\lambda_1^{-\alpha_i} + \lambda_2^{-\alpha_i} + \lambda_3^{-\alpha_i} - 3\right) + \sum_{i=1}^{N} \frac{1}{D_i}(J_{el} - 1)^{2i} \qquad (2)$$

Where μ_i, α_i, N, and D_i are the material constants, $\lambda_j^{-\alpha_i}$ are the deviatoric stretches, and and J_{el} is the elastic volume ratio.

The material constant for the Neo-Hookean and the Ogden model provided in the table 1.

Table 1. Material constants for the Neo-Hookean and the Ogden model

S.No.	Hyperelastic Material Model	Material Constants

1	Neo-Hookean	$C_{10} = 2587.7$ kPa, and $D_1 = 0.0001$
2	Ogden	$\mu_1 = 445.1$ kPa, $\alpha_1 = -224.1$, and $D_1 = 0.0001$ $\mu_2 = 3289.8$ kPa, $\alpha_2 = 4375.3$, and $D_1 = 0.0001$ $\mu_3 = 2891.7$ kPa, $\alpha_3 = -278.3$, and $D_1 = 0.0001$

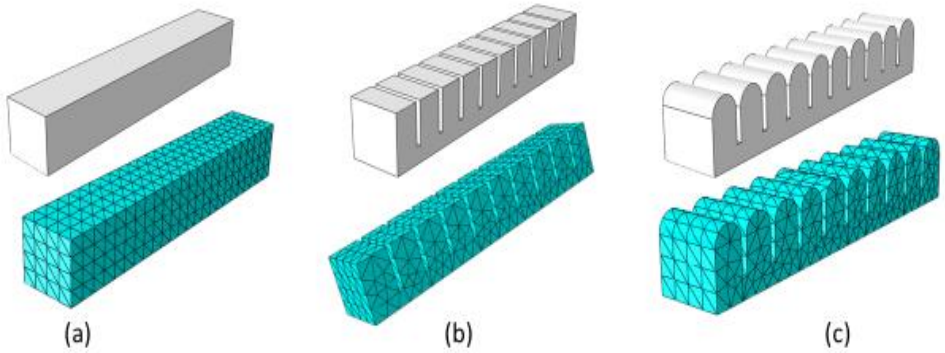

Figure 4. Three different SPA models along with their meshing

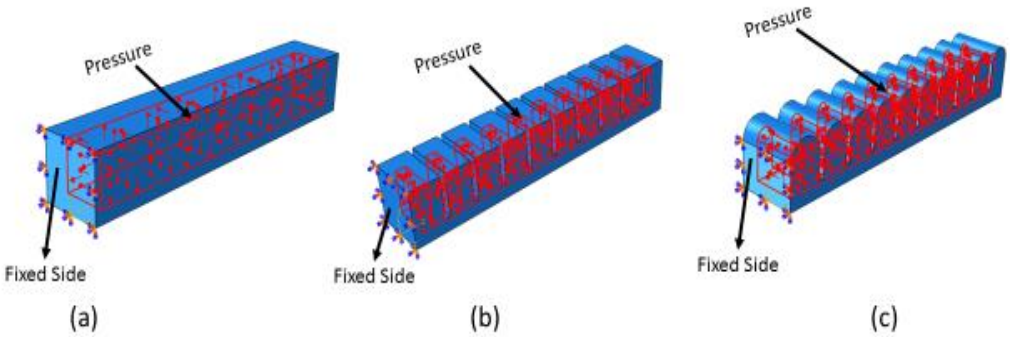

Figure 5. The boundary and loading condition for the SPAs

For the computation analysis the design software Abaqus has been considered. The IGES file of the SPAs are imported into the Abaqus. The three-dimensional model is meshed using the tetrahedral type element with hybrid formulation (figure 4). The total number of elements for the single chamber SPA with rectangular cross-section, multi-chamber SPA with square air chambers, and multi-chamber SPA with circular air chambers are 2098, 3358, and 3717, respectively. For the boundary condition, all the SPAs are considered to be fixed at one side and other side is free to deform (figure 5).

4. Results and Discussion

The analysis is carried out using the finite element analysis (FEA) theory. The SPAs are actuated with the pneumatic pressure of 32 kPa using the Neo-Hookean and the Ogden hyperelastic model. Using the Neo-hookean model, the single chamber SPA with

rectangular cross-section creates a bending of approximately 5^0 at 26 kPa (figure 7a). Similarly, at 26 kPa, the multi-chamber SPA with square and circular air chambers creates a bending of approximately 170^0 and 177^0, respectively (figure 6 b&c). The bending created by the three different SPAs is shown in the figure 6.

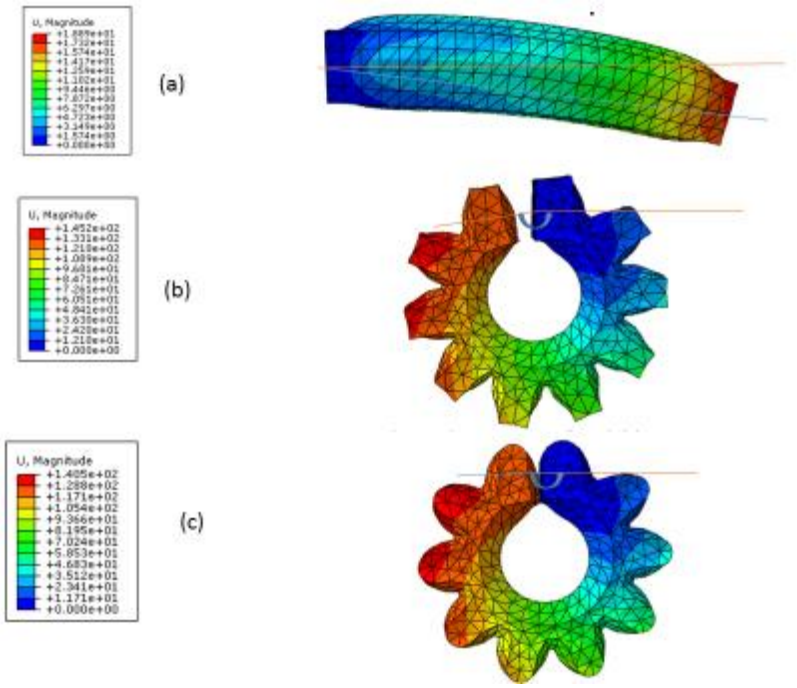

Figure 6. Bending of (a) single chamber SPA with rectangular cross-section, (b) multi-chamber SPA with square air chambers, and (c) multi-chamber SPA with circular air chambers at 32 kpa pneumatic pressure using the Neo-Hookean model.

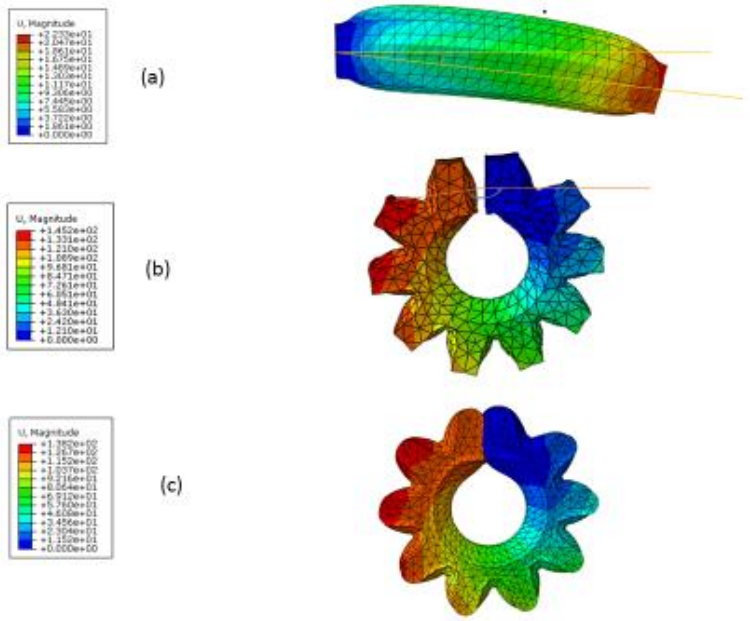

Figure 7. Bending of (a) single chamber SPA with rectangular cross-section, (b) multi-chamber SPA with square air chambers, and (c) multi-chamber SPA with circular air chambers at 32 kpa pneumatic pressure using the Ogden model.

Similarly, Using the Ogden model, the single chamber SPA with rectangular cross-section creates a bending of approximately 6^0 at 32 kPa (figure 7a). Similarly, at 32 kPa, the multi-chamber SPA with square and circular air chambers creates a bending of approximately 175^0 and 180^0, respectively (figure 7 b&c).

Table 2. Deformation and bending of the SPAs at 26 and 32 kPa pneumatic pressure

S. No.	Type of SPA	Actuating Pressure (32 kPa)			
		Neo-Hookean Model		Ogden Model	
		Bending (^{0})	Deformation (mm)	Bending (^{0})	Deformation (mm)
1	Single chamber SPA (rectangular cross-section)	5	18.8	6	23.3
2	Multi-chamber SPA (square air chambers)	170	14.5	175	14.5
3	Multi-chamber SPA (circular air chambers)	177	14	180	13.8

From figures 6&7, it can be observed that the SPA with a single chamber creates a very low bending angle as compared to the SPAs with multiple chambers. This is due to the radial expansion of the single chamber, also known as the ballooning effect. This radial expansion is not able to create a high bending moment on the lower layer, thus, leading to smaller bending. Whereas the presence of multiple air chambers separated by a small gap between them eliminates the ballooning effect. The small gap allows the SPA to bend easily and even create higher bending at low pneumatic pressures. However, SPA with circular air chambers creates larger bending as compared to the SPA with a square air chambers. This is because the SPA with square air chambers has different wall stiffness (the top wall has low stiffness as compared to the side wall). Due to low stiffness, the top wall suffers high expansion as compared to the side wall and creates a bending moment on the lower layer. But in the case of SPA with circular air chambers, the top and side wall has the same stiffness because of the same thickness. This led to the equal expansion of the circular air chambers and develops a higher bending moment on the lower layer as compared to the air chambers with the square air chambers.

5. Conclusion

The conducted study uses the FEA theory to evaluate the hyperelastic material model for bending of the SPAs. The analysis results concluded that the SPA with multiple air chambers creates higher bending angle as compare to the SPA with singe chamber under similar boundary loading condition. However, the multiple chambers SPA with circular

air chambers creates higher bending as compared to the multiple chambers SPA with square air chambers under similar boundary and loading conditions. Moreover, the Ogden model results are better than the Neo-Hookean results in terms of bending.
On the basis of FEA results, one can say that the Ogden model is better than the Neo-Hookean model for analyzing SPA fabricated with natural rubber that are subjected to the higher strains.

References:

1. Hu, W., Mutlu, R., Li, W., & Alici, G. (2018). A structural optimisation method for a soft pneumatic actuator. robotics, 7(2), 24.
2. Alici, G., Canty, T., Mutlu, R., Hu, W., & Sencadas, V. (2018). Modeling and experimental evaluation of bending behavior of soft pneumatic actuators made of discrete actuation chambers. Soft robotics, 5(1), 24-35.
3. Gariya, N., & Kumar, P. (2022). A comparison of plane, slow pneu-net, and fast pneu-net designs of soft pneumatic actuators based on bending behavior. Materials Today: Proceedings.
4. Suh, C., Margarit, J. C., Song, Y. S., & Paik, J. (2014, September). Soft pneumatic actuator skin with embedded sensors. In 2014 IEEE/RSJ International Conference on Intelligent Robots and Systems (pp. 2783-2788). Ieee.
5. El-Agroudy, M. N., Gaber, M., Joseph, D., Ibrahim, M., Amin, M., Helmy, D., ... & Maged, S. A. (2020, February). Assistive exoskeleton hand glove. In 2020 International Conference on Innovative Trends in Communication and Computer Engineering (ITCE) (pp. 164-169). IEEE.
6. Gariya, N., Kumar, P., & Prasad, B. (2022). Stress and bending analysis of a soft pneumatic actuator considering different hyperelastic materials. Materials Today: Proceedings.
7. Renda, F., Giorelli, M., Calisti, M., Cianchetti, M., & Laschi, C. (2014). Dynamic model of a multibending soft robot arm driven by cables. IEEE Transactions on Robotics, 30(5), 1109-1122.
8. Della Santina, C., Bicchi, A., & Rus, D. (2020). On an improved state parametrization for soft robots with piecewise constant curvature and its use in model based control. IEEE Robotics and Automation Letters, 5(2), 1001-1008.
9. Renda, F., Armanini, C., Lebastard, V., Candelier, F., & Boyer, F. (2020). A geometric variable-strain approach for static modeling of soft manipulators with tendon and fluidic actuation. IEEE Robotics and Automation Letters, 5(3), 4006-4013.
10. Bauchau, O. A., & Craig, J. I. (2009). Euler-Bernoulli beam theory. In Structural analysis (pp. 173-221). Springer, Dordrecht.
11. Moseley, P., Florez, J. M., Sonar, H. A., Agarwal, G., Curtin, W., & Paik, J. (2016). Modeling, design, and development of soft pneumatic actuators with finite element method. Advanced engineering materials, 18(6), 978-988.

12. Sedal, A., Bruder, D., Bishop-Moser, J., Vasudevan, R., & Kota, S. (2018). A continuum model for fiber-reinforced soft robot actuators. Journal of Mechanisms and Robotics, 10(2), 024501.
13. Bishop-Moser, J., & Kota, S. (2015). Design and modeling of generalized fiber-reinforced pneumatic soft actuators. IEEE Transactions on Robotics, 31(3), 536-545.
14. Marchese, A. D., Onal, C. D., & Rus, D. (2014). Autonomous Soft Robotic Fish Capable of Escape Maneuvers using Fluidic Elastomer Actuators," Soft Robotics, vol. 1, no. 1.
15. Hassan, T., Manti, M., Passetti, G., d'Elia, N., Cianchetti, M., & Laschi, C. (2015, August). Design and development of a bio-inspired, under-actuated soft gripper. In 2015 37th Annual International Conference of the IEEE Engineering in Medicine and Biology Society (EMBC) (pp. 3619-3622). IEEE.
16. Kim, B., Lee, S. B., Lee, J., Cho, S., Park, H., Yeom, S., & Park, S. H. (2012). A comparison among Neo-Hookean model, Mooney-Rivlin model, and Ogden model for chloroprene rubber. International Journal of Precision Engineering and Manufacturing, 13(5), 759-764.